

MASS-TO-LIGHT RATIOS OF GALAXY GROUPS FROM WEAK LENSING

LAURA C. PARKER^{1 2} AND MICHAEL J. HUDSON¹

Department of Physics, University of Waterloo, Waterloo, ON, N2L 3G1

R.G. CARLBERG

Department of Astronomy & Astrophysics, University of Toronto, Toronto, ON, M5S 3H8

AND

HENK HOEKSTRA

Department of Physics and Astronomy, University of Victoria, Victoria, BC, V8W 2Y2

Draft version October 16, 2018

ABSTRACT

We present the findings of our weak lensing study of a sample of 116 CNOC2 galaxy groups. The lensing signal is used to estimate the mass-to-light ratio of these galaxy groups. The best fit isothermal sphere model to our lensing data has an Einstein radius of $0''.88 \pm 0''.12$, which corresponds to a shear-weighted velocity dispersion of $245 \pm 18 \text{ km s}^{-1}$. The mean mass-to-light ratio within $1 \text{ h}^{-1} \text{ Mpc}$ is $185 \pm 28 \text{ hM}_\odot/L_{B\odot}$ and is independent of radius from the group center.

The signal-to-noise ratio of the shear measurement is sufficient to split the sample into subsets of “poor” and “rich” galaxy groups. The poor galaxy groups were found to have an average velocity dispersion of $193 \pm 38 \text{ km s}^{-1}$ and a mass-to-light ratio of $134 \pm 26 \text{ hM}_\odot/L_{B\odot}$, while the rich galaxy groups have a velocity dispersion of $270 \pm 39 \text{ km s}^{-1}$ and a mass-to-light ratio of $278 \pm 42 \text{ hM}_\odot/L_{B\odot}$, similar to the mass-to-light ratio of clusters. This steep increase in the mass-to-light ratio as a function of mass, suggests that the mass scale of $\sim 10^{13} \text{ M}_\odot$ is where the transition between the actively star-forming field environment and the passively-evolving cluster environment occurs. This is the first such detection from weak lensing.

Subject headings: gravitational lensing, galaxy groups, dark matter, mass-to-light ratios, galaxy halos

1. INTRODUCTION

Galaxy groups dominate the overall mass and luminosity densities of the Universe yet their properties are poorly understood in comparison to individual galaxies or rich galaxy clusters. Until now galaxy groups have not been extensively used for cosmology largely because they are notoriously difficult to identify due to their small contrast with the field. However, with large redshift surveys it is now possible to identify substantial samples of galaxy groups.

A sample of roughly 200 galaxy groups was identified in the Canadian Network for Observational Cosmology 2 (CNOC2) redshift survey using an iterative friends-of-friends algorithm (Carlberg et al. 2001). The dynamical analysis of these groups indicated a rising mass-to-light ratio with radius. This suggests that groups are the scale where segregation begins to occur between mass and light. This effect could be due to dynamical friction, or to a large core radius which could indicate that dark matter has different properties from “standard” collisionless cold dark matter (CDM). The cores of galaxies and clusters appear to be less cuspy than expected, which

has prompted theoretical work in alternative dark matter models (see discussion in Governato et al. 2001).

The dark matter density profile has yet to be measured for galaxy groups. Dynamical studies of groups are difficult because kinematic information is known for very few galaxies, and because equilibrium assumptions might not be valid. Furthermore, these difficulties increase at large radii from the group center. Weak gravitational lensing has proven invaluable in the analysis of single massive objects such as galaxy clusters (Hoekstra et al. 1998; Mellier 1999) as well as in the statistical studies of individual galaxies (Brainerd, Blandford & Smail, 1996; Hudson et al. 1998; Fischer et al. 2000; Sheldon et al. 2001; Hoekstra et al. 2004). To date there has been only one weak lensing measurement of galaxy groups (Hoekstra et al. 2001) using a small subsample of the total CNOC2 galaxy group catalog.

Assuming that the dark matter halos of groups are well described by an isothermal sphere, we expect a tangential shear signal as follows

$$\gamma_T = \frac{\theta_E}{2\theta} = \frac{4\pi\sigma^2}{c^2} \frac{D_{LS}}{D_S} \quad (1)$$

where σ is the velocity dispersion of the halo, and D_S and D_{LS} are the angular diameter distances to the source and between lens and source, respectively.

The intent of this paper is to present the results of our weak lensing study of CNOC2 galaxy groups and to compare these results with those found from the dynamical measurements (Carlberg et al. 2001) and the weak lensing detection of Hoekstra et al. (2001). We

¹ Visiting Astronomer, Kitt Peak National Observatory, National Optical Astronomy Observatory, which is operated by the Association of Universities for Research in Astronomy, Inc. (AURA) under cooperative agreement with the National Science Foundation

² Based on observations obtained at the Canada-France-Hawaii Telescope (CFHT) which is operated by the National Research Council of Canada, the Institut National des Sciences de l’Univers of the Centre National de la Recherche Scientifique of France, and the University of Hawaii.

will also present the results when the sample of groups is split into two samples of “rich galaxy groups” and “poor galaxy groups”, divided by velocity dispersion. A second paper will follow with the results of galaxy-galaxy lensing in these fields and a maximum likelihood analysis of the shear.

2. DATA

2.1. CNOC2 Groups

Our galaxy group catalogs were generated using a friends-of-friends algorithm with the CNOC2 redshift survey data (Yee et al. 2000; Carlberg et al. 2001). The CNOC2 area contains 4 fields well-spaced in right ascension and was intended to better understand the properties of field galaxies. The CNOC2 galaxy sample contains 6200 galaxies with redshifts to z of 0.7. From this galaxy catalog a sample of 192 galaxy groups was identified. The average number of galaxies identified in each group is ~ 4 and the groups have a median redshift of 0.33. The groups have a median dynamically determined velocity dispersion of 190 km s^{-1} .

2.2. Observations

For this project we observed the 4 central patches of the CNOC2 fields, where most of the galaxy groups are located. The observations were carried out mostly at the Canada-France-Hawaii Telescope with 2 additional nights at the Kitt Peak National Observatory Mayall 4-m Telescope. The fields were observed in B,V, R_c , and I_c . Deep exposures (~ 4 hours) were taken in the R_c and I_c bands, which were used for the lensing measurements. The characteristics of the data obtained are outlined in Table 1.

2.3. Reduction/Stacking

Gravitational lensing is usually limited by systematics and it is important to ensure no spurious shear is introduced in the stacking procedure. This can be achieved by carefully monitoring the astrometry over each input image that enters the stack. Wide-field cameras in use today have larger distortions than earlier, smaller CCD cameras. This distortion must be properly mapped and corrected in order to ensure no artificial source of shear is imported during the stacking process. Note, however, that group lensing is less affected by systematics than cosmic shear studies (the weak lensing signal from the large scale structure in the Universe). This is due to the random orientation of the galaxy-group pairs across the field, as opposed to looking for a preferred orientation as cosmic shear studies do. Cosmic shear measurements use the patterns in the large-scale distortion field of background sources to map out the matter distribution in the Universe. This signal is tiny and more susceptible to systematics than galaxy-galaxy or group-galaxy lensing where the shear signal is averaged in radial bins around each lens. In this analysis the image reduction and stacking was carried out using the IRAF mosaic package *mscred* (Valdes, F.G., 1997).

2.4. Object Detection and Shape Parameters

Object catalogs were extracted from our stacked images using the *imcat* software, an implementation of the Kaiser, Squires and Broadhurst (1995, hereafter KSB)

method. This software is optimized for measuring the shapes of faint sources. The object detection algorithm works by smoothing the images using different sized filters and then detecting the “peaks” which are then added to the source catalog. For each detected object weighted quadrupole moments were measured and the resulting polarizations were calculated:

$$e_1 = \frac{I_{11} - I_{22}}{I_{11} + I_{22}} \text{ and } e_2 = \frac{2I_{12}}{I_{11} + I_{22}} \quad (2)$$

The polarization measurements need to be corrected for the effects of seeing, camera distortion and PSF anisotropy. These corrections to correct for these concerns have been discussed in KSB and Luppino & Kaiser (1997) with some improvements made by Hoekstra et al. (1998 and 2000). The techniques work well for ground-based data where the PSF is stable and not very anisotropic, and where the fields contain many stars which are used in the correction algorithms. The source catalogs are trimmed so that all stars are removed. The stars can easily be located by comparing magnitude and half light radius. We kept only those objects for which the half light radii were greater than 1.2 times the stellar PSF, thus ensuring the contamination from stars in our source catalog is very small. The limiting magnitude of our images is approximately 25 in R_c .

3. ANALYSIS

3.1. Weak Lensing Measurement

In the weak lensing analysis we used a source catalog of approximately 150 000 objects (~ 40 per sq arcminute) and a galaxy group catalog containing the 116 CNOC2 galaxy group centers that were within the area we observed. The faint members of the galaxy groups are included in the source catalog, but as shown by Hoekstra et al. (2001), this does not contaminate the final result. This is indicated by the fact that the number density of faint galaxies does not increase significantly towards the group center, thus faint group members do not influence the final shear measurement.

The source density of background objects is not sufficiently high to extract a signal from individual galaxy groups, except for the most massive groups, and so the galaxy groups must be stacked and the weak lensing signal measured around the stacked groups. The source galaxies around the stacked galaxy group were divided into radial bins and the average distortion was calculated in each bin. The component of the average distortion tangential to the group center is the weak lensing signal and is displayed in Figure 1a. The tangential shear is plotted in physical bins (units of $h^{-1}\text{Mpc}$) since the redshift of each galaxy group is precisely known from the CNOC2 redshift survey. Using equation (1), the best fit isothermal sphere to the average tangential shear profile yielded an Einstein radius of $0''.88 \pm 0''.13$.

We can alternatively fit the tangential shear data with a Navarro, Frenk and White (NFW) dark matter profile (Navarro, Frenk & White, 1996). This density profile, which has been observed to fit mass distributions well over a wide range of scales, is given by

$$\rho(r) = \frac{\delta_c \rho_c}{(r/r_s)(1 + r/r_s)^2} \quad (3)$$

where ρ_c is the critical density for closure of the Universe. The scale radius, r_s , is defined as r_{200}/c where c

TABLE 1
FIELD INFORMATION.

Field	RA (2000)	DEC (2000)	Telescope	Area sq.arcmin	Source Density (No./sq arcmin)	Median Seeing	No. of Groups
0223	36.51992	0.3116	KPNO	1120	30	1.1	23
0920	140.95504	37.0861	CFHT	1100	45	0.9	40
1447	222.4096	9.13883	CFHT	1220	32	0.8	29
2148	327.8317	-5.5586	CFHT	1125	44	0.8	25

is the dimensionless concentration parameter, and δ_c is the characteristic over-density of the halo. The tangential shear signal γ_T as a function of radius θ for a NFW halo is given by (Wright & Brainerd, 2000).

We use the tangential shear data to do a one-parameter fit to the NFW profile, while assuming a reasonable value for the concentration parameter, c . Based on the high resolution numerical simulations of Bullock et al. (2001), a concentration parameter of ~ 10 was used as an estimate for galaxy group scales. The best fit NFW profile can be seen as the dashed line in Fig 1a. Over the scales where we can measure the weak lensing signal the NFW profile and the isothermal sphere are very similar and are both good fits to the data. The similarity of these two models at the galaxy group mass scale is expected from models (Wright & Brainerd, 2000).

A common systematic test employed in gravitational lensing is to measure the signal when the phase of the distortion is increased by $\pi/2$. If the measured tangential distortion is due to gravitational lensing the rotated signal should be consistent with 0 as is shown in Figure 1b. In addition to the standard systematic test, we also measured the signal around random points in the field. This test yielded no signal which indicates the results plotted in Figure 1a are indeed due to gravitational lensing by the groups.

3.2. Velocity Dispersion

In order to relate our estimate of the Einstein radius to the average velocity dispersion of the groups, the redshift distribution of the background sources must be understood. The strength of the gravitational lensing signal as a function of redshift is characterized by the parameter β which is defined as $\beta = \max[0, D_{LS}/D_S]$ where D_{LS} is the angular diameter distance between the lens and the source and D_S is the angular diameter distance from the observer to the source. β was calculated for each group-source pair based on the known spectroscopic redshift of the group and the estimated redshift of the source. The source redshift estimate was based on the observed R_c magnitude and the method outlined in Brainerd, Blanford and Smail (1996). We find a value of $\beta = 0.49$. This yields an ensemble averaged group velocity dispersion $\langle \sigma^2 \rangle^{1/2} = 245 \pm 18 \text{ km s}^{-1}$ for an $\Omega_m = 0.3$, $\Omega_\Lambda = 0.7$ universe. This value agrees well with Hoekstra et al. (2001) who found $\langle \sigma^2 \rangle^{1/2} = 258 \pm 50 \text{ km s}^{-1}$ for an $\Omega_m = 0.2$, $\Omega_\Lambda = 0.8$ universe, although our result has considerably smaller errors. Our measured velocity dispersion from weak lensing also agrees with the results from a dynamical study of the CNOC2 groups (Carlberg et al. 2001) who found $\sigma \sim 200 \text{ km s}^{-1}$.

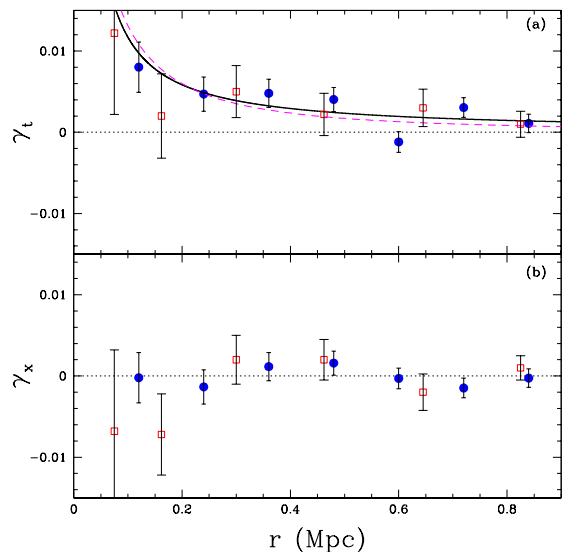


FIG. 1.— (a) The ensemble averaged tangential shear as a function of radius around a sample of CNOC2 galaxy group centers from Carlberg et al. (2000). The best fit isothermal sphere, shown with the solid line, yields an Einstein radius of $0''.88 \pm 0''.13$ corresponding to a velocity dispersion of $245 \pm 18 \text{ km s}^{-1}$. The best fit NFW profile is shown with the dashed curve. (b) The signal when the phase is rotated by $\pi/2$. No signal is present as expected if the signal in (a) is due to gravitational lensing. The results of Hoekstra et al. (2001) are shown with the open squares while the results of this paper are shown with filled circles. There is good agreement between the two measurements but the result here is a much more significant detection

3.3. Mass-to-Light Ratio

Gravitational lensing can be used to estimate masses, and hence mass-to-light ratios. The mass estimate comes directly from the isothermal sphere fit to the tangential shear data, and the light information comes from the CNOC2 galaxy catalogs (Yee et al. 2000). Each galaxy in the redshift survey has a measured magnitude and various weights (color, geometric and redshift) to account for incompleteness in the sample. The galaxy group luminosity profile was calculated by using the magnitudes and weights for each galaxy that belonged to a galaxy group. The galaxies were placed in radial bins centered at the group centers, just as was done to measure the lensing signal. The luminosity of each galaxy was calculated, with a correction for galaxies fainter than the survey limit. This was done by employing the CNOC2 galaxy luminosity function published in Lin et al. (1999) and using the spectral classification provided in the CNOC2 galaxy catalogs. The luminosities were not corrected for evolution, but were k-corrected. The mass-to-light ratio

of the galaxy groups as a function of radius is plotted in Figure 2. We obtain an integrated mass-to-light ratio to $1.0 h^{-1} \text{Mpc}$ of $185 \pm 28 h M_{\odot}/L_{B\odot}$, consistent with the value of $191 \pm 81 h M_{\odot}/L_{B\odot}$ found by Hoekstra et al. (2001) using a subset of the groups. The method employed by Hoekstra et al. was slightly different in that the mass-to-light ratio was estimated by calculating the ratio between the measured shear signal and the expected shear derived from the luminosity profile. This method requires the assumption that the mass-to-light ratio is constant across the groups and was necessary because of the smaller data set and low signal-to-noise ratio. As is clear in Figure 2, the M/L is remarkably flat as a function of distance from the group center. This is in contrast to what was found by the dynamical study of the CNOC2 groups, as will be discussed in Section 4. If the M/L is calculated using the NFW mass profile the results are statistically equivalent.

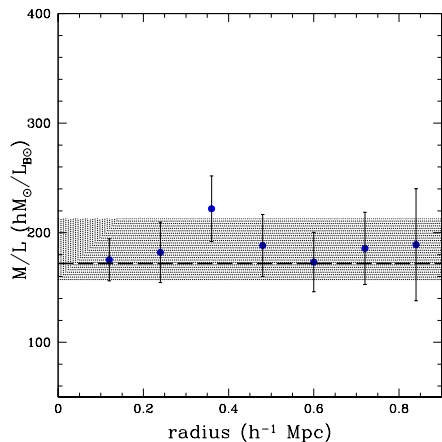


FIG. 2.— The mass-to-light ratio for the entire sample of galaxy groups in radial bins. The average M/L is $185 \pm 28 h M_{\odot}/L_{B\odot}$. The hatched region represents the $1\text{-}\sigma$ bounds on the mass-to-light ratio, assuming M/L is constant with radius. The heavy dashed line indicates the M/L calculated using all CNOC2 galaxies projected to be close to the galaxy group center, as described in the text.

It is important to note that the tangential shear signal is sensitive to all matter along the line-of-sight, and as the distance from the group center increases more of the signal is coming from other mass that is correlated with the group (like a 2-halo term in a cross-correlation function). In addition to calculating the M/L of the galaxy groups using the known group members from the CNOC2 groups catalog, we also calculated the M/L for all galaxies in the CNOC2 galaxy catalog projected to be within a small distance of the group center (1200 km s^{-1} along the line-of-sight). The mass model does not change but the luminosity profile is altered by including more galaxies. The total M/L is lower by 8%, which is within the 1σ errors, and is still flat with distance from the group center. Assuming a constant M/L with distance from the group center, the best fit M/L using this larger sample of galaxies can be observed as the heavy dashed line in Figure 2.

3.4. Mass-to-Light Ratios of Rich and Poor Galaxy Groups

We wanted to examine the difference in the shear signal from the rich and poor groups, and to this end we divided

the galaxy group catalog into two subsamples. We split the sample by the median dynamical velocity dispersion (190 km s^{-1}), although results were similar regardless of whether the groups were divided by their luminosities or velocity dispersions. The same source catalog was used to study the two group subsets. The only difference from the technique outlined in the sections above is that the input group catalogs have half the number of groups. The resulting tangential and cross shear for the two group subsets are shown in Figure 3.

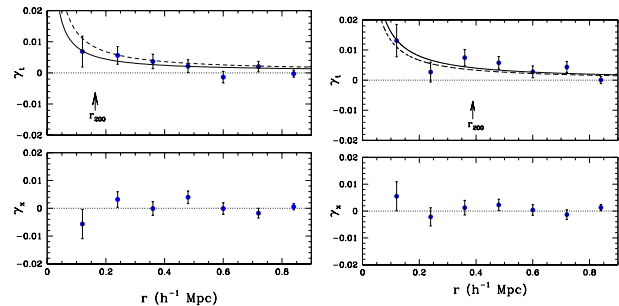


FIG. 3.— The tangential and cross components of shear as in Figure 1, on the left for the sample of “poor” groups, which have dynamical velocity dispersions less than 190 km s^{-1} , and on the right for the “rich” galaxy groups, which have velocity dispersions greater than 190 km s^{-1} . The best fit isothermal sphere is plotted with a solid line in both plots. The best fit velocity dispersion is $193 \pm 38 \text{ km s}^{-1}$ for the poor groups and $270 \pm 39 \text{ km s}^{-1}$ for the rich groups. The dashed line is the best fit isothermal sphere from Figure 1, for the entire data set. The characteristic r_{200} values (Carlberg et al. 2001) are indicated by the arrow.

The results clearly indicate that the lensing signal is dominated by the larger groups. A few of the galaxy groups identified in the CNOC2 fields had measured velocity dispersions in excess of 500 km s^{-1} . To be certain that the tangential shear signal measured was not coming solely from these groups we measured the tangential shear around only those groups with velocity dispersions greater than 500 km s^{-1} . In addition, we also repeated the measurement of the tangential shear around all galaxies except those with velocity dispersions greater than 500 km s^{-1} . The results indicated that there is a substantial signal coming from the most massive galaxy groups (small clusters) but that the tangential shear profile is not dominated by these for the sample as a whole. After the massive groups are removed an isothermal tangential shear profile with an Einstein radius of roughly $0.8''$ remains.

The shear profiles for the two subsamples were fit with isothermal spheres and their mass-to-light ratios were estimated. The mean velocity dispersion of the “poor” groups is $\langle \sigma^2 \rangle^{1/2} = 193 \pm 38 \text{ km s}^{-1}$, while the “rich” groups have a velocity dispersion of $\langle \sigma^2 \rangle^{1/2} = 270 \pm 39 \text{ km s}^{-1}$. The mass-to-light ratios of the “rich” and “poor” galaxy groups are flat with radius, as can be seen in Figure 4. The weighted mean mass-to-light ratio of the “poor” groups is $134 \pm 26 h M_{\odot}/L_{B\odot}$, while the mass-to-light ratio of the “rich” groups is $278 \pm 42 h M_{\odot}/L_{B\odot}$. Once again, the M/L s were also calculated using a catalog of galaxies projected to be close to the group center and the best fit results are shown with the heavy dashed lines in Figure 4.

4. DISCUSSION

Weak lensing is a powerful tool for understanding the ensemble-averaged properties for a sample of objects, but can not tell us about the properties of an individual galaxy group. It is of great interest to compare the results we obtained for our sample of CNOC2 galaxy groups to those obtained by Carlberg et al. (2001), using dynamical methods on the full sample of CNOC2 galaxy groups. In Figure 5 we have plotted the mass-to-light ratio of galaxy groups as a function of radius from the lensing, as well as the best fit curve for the dynamical data. Note that the M/L ratio is plotted in units of r_{200} . Our values for the r_{200} for each group came from the Carlberg et al. galaxy group catalog. We repeated the complete analysis of the shear and of the luminosity based in units of r_{200} . We do not observe the steep increase in M/L that was observed with the dynamical methods, and our data can be well-fit with a straight line with no slope. The M/L calculated from the dynamical data is dependent on the orbits of the galaxies in the groups, but their result of a rising M/L is robust for all reasonable orbits. The lensing- and dynamically-derived properties of these CNOC2 groups are outlined in Table 2.

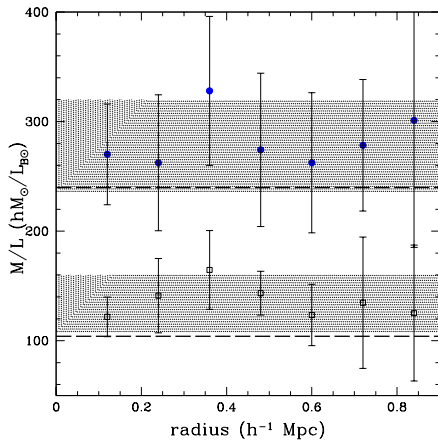


FIG. 4.— The mass-to-light ratio for subsamples of galaxy groups in radial bins. Symbols are as in Figure 2. The mass-to-light ratio of the poor galaxy groups (open squares) and rich galaxy groups (filled circles) as a function of the distance from the group center. The average M/L of the rich groups is $278 \pm 42 \text{ hM}_\odot/L_{B0}$ and $134 \pm 26 \text{ hM}_\odot/L_{B0}$ for the poor groups. There is a clear offset in the mass-to-light ratio for the two subsamples as can be seen by comparing the two hatched regions.

It is particularly interesting to plot our two values for the mass-to-light ratio of galaxy groups on the mass sequence, and compare our results to previous measurements. This can be seen in Figure 6 where B-band mass-to-light ratios for galaxy groups and clusters are plotted. The curve is from Marinoni & Hudson (2002), who estimated the mass-to-light ratio by comparing the mass function from Press-Schechter theory with their measured luminosity function of virialized systems. Our data follow the trend of rising mass-to-light ratio with mass. We are in approximate agreement with the global mass-to-light ratio found on similar scales by Carlberg et al. (2001), Tucker et al. (2000) and Eke et al. (2004), although some of these studies are at a lower redshift.

The halo mass of approximately $10^{13} M_\odot$, hosting typically 3 L^* galaxies (Marinoni & Hudson 2002), appears to be a critical scale, at which the mass-to-light

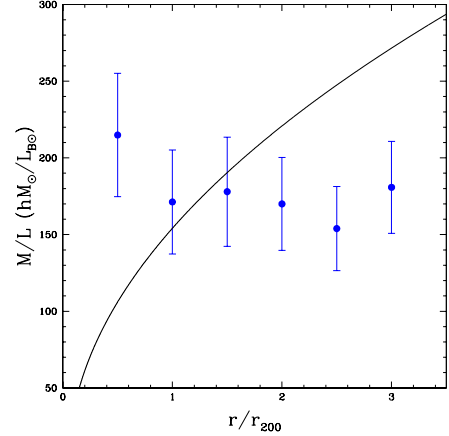


FIG. 5.— The mass-to-light ratio of the galaxy groups in radial bins in units of r_{200} . The line is fit to the dynamical results of Carlberg et al. (2001). We do not observe the steep rise in mass-to-light ratio with radius. Note that the Carlberg et al. results are for a 3-dimensional mass-to-light ratio while the data points are in projection.

ratio is increasing dramatically as a function of mass. This could indicate the transition from the actively star-forming field environment to the passively-evolving-galaxy-dominated cluster regime. Note that the M/L of the rich galaxy groups appears to be comparable to that found in massive galaxy clusters (Carlberg et al. 1997), as seen in Figure 6, so there is presumably little change in M/L on more massive scales.

A rise in M/L on these scales has been suggested previously, from analysis based directly on dynamical studies of groups (Marinoni & Hudson 2002; van den Bosch, Yang and Mo 2003; Eke et al. 2004) and from semi-analytic models (for example Benson et al. 2000), see also discussion in Dekel & Birnboim (2004). The results of this paper are then consistent with previous studies, although this weak lensing result suggests a somewhat steeper increase than had been found previously.

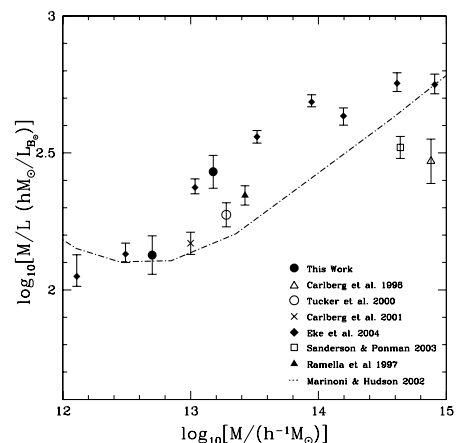


FIG. 6.— The mass-to-light ratio as a function of mass for samples of groups and clusters from the literature. The curve (Marinoni & Hudson, 2002) is generated by comparing the mass function from Press-Schechter theory for a Λ CDM universe with an observed luminosity function. Note that the different samples span a range of redshifts. For example, our median redshift is 0.33 while the 2PIGG data (Eke et al. 2004) median redshift is roughly 0.1.

From the average mass-to-light ratio for our entire sam-

TABLE 2
WEAK LENSING AND DYNAMICAL PROPERTIES OF GALAXY GROUPS

Sample	mean N_{gal} per group	$\langle \sigma \rangle^{lensing}$ $km\ s^{-1}$	$\langle \sigma \rangle^{dyn\ a}$ $km\ s^{-1}$	$\langle M/L \rangle_B$ hM_{\odot}/L_{\odot}	median redshift
all groups	3.9	245 ± 18	219 ± 10	185 ± 28	0.323
rich groups	4.2	270 ± 38	311 ± 13	278 ± 42	0.360
poor groups	3.6	198 ± 38	127 ± 4	134 ± 26	0.303

^aCarlberg et al. 2001

ple of galaxy groups it is possible to naively estimate Ω_m using the method outlined in Carlberg et al. (1997). By combining M/L with luminosity density it is possible to estimate the matter density of the Universe.

$$\Omega_m = \frac{\rho_m}{\rho_c} = \frac{\rho_L}{\rho_c} \frac{M}{L} \quad (4)$$

Using a mass-to-light ratio of $185 \pm 28\ hM_{\odot}/L_{R\odot}$ (converted to $hM_{\odot}/L_{AB\odot}$), and the luminosity density for CNOC2 galaxies found in Lin et al. (1999) we obtain $\Omega_m = 0.22 \pm 0.06$. This is a valid estimate of Ω_m only if galaxy groups dominate the mass and luminosity of the Universe. In order to properly calculate Ω_m , it is necessary to know the mass-to-light function for a wide range of masses, extending to single galaxies and rich clusters.

5. CONCLUSIONS

We have detected a significant weak lensing signal for a sample of 116 intermediate redshift galaxy groups. From the lensing signal we estimate that galaxy groups have a mean M/L of $185 \pm 28\ hM_{\odot}/L_{B\odot}$ within $1\ h^{-1}Mpc$, and

that this M/L is constant as the distance from the group center increases. When the sample is split into subsets of rich and poor galaxy groups, there is a clear offset in the mass-to-light ratios of the two subsets. The increase in the M/L as a function of mass is in general agreement with other results, but is detected here for the first time using weak lensing in the galaxy group mass regime.

This analysis indicates that a weak lensing signal can indeed be measured from galaxy groups. Clearly, a larger sample with well determined dynamical properties would be ideal for this sort of study. The structure of the dark matter halos of galaxy groups are still poorly understood. By combining this group lensing result with galaxy-galaxy lensing it should be possible to determine the size and extent of galaxy group dark matter halos, which will aid significantly in our understanding of structure in the Universe and the nature of dark matter.

MJH acknowledges support from NSERC and a Premier's Research Excellence Award.

REFERENCES

- Benson, A. J., Cole, S., Frenk, C. S., Baugh, C. M., Lacey, C. G., 2000, MNRAS, 311, 793
 Brainerd, T. G., Blandford, R. D., Smail, I., 1996, ApJ, 466, 623
 Bullock, J.S. et al., 2001, MNRAS, 321, 559
 Carlberg, R. G., Yee, H. K. C., Ellingson, E.; Abraham, R., Gravel, P., Morris, S., Pritchet, C. J., 1996, ApJ, 462, 32
 Carlberg, R. G., Yee, H. K. C., Ellingson, E., 1997, ApJ, 478, 462
 Carlberg, R. G., Yee, H. K. C., Morris, S. L., Lin, H., Hall, P. B., Patton, D. R., Sawicki, M., Shepherd, C. W., 2001, ApJ, 552, 427
 Dekel, Avishai, Birnboim, Yuval, 2004, astro-ph/0412300
 Eke, V.R., et al., 2004, MNRAS, 355, 769
 Fischer, P. et al., 2000, AJ120, 1198
 Governato, F., Ghigna, S., Moore, B., Quinn, T., Stadel, J., Lake, 2001, ApJ, 547, 555
 Hoekstra, H., Franx, M., Kuijken, K., Squires, G., 1998, ApJ, 504, 636
 Hoekstra, H., Franx, M., Kuijken, K., 2000, ApJ, 532, 88
 Hoekstra, H., Franx, M., Kuijken, K., Carlberg, R. G., Yee, H. K. C., Lin, H., Morris, S. L., Hall, P. B., Patton, D. R., Sawicki, M., Wirth, G. D., 2001, ApJ, 548, 5
 Hoekstra, H., Yee, H. K. C., Gladders, M. D., 2004, ApJ, 606, 67
 Hudson, M. J., Gwyn, S. D. J., Dahle, H., Kaiser, N., 1998, ApJ, 503, 531
 Kaiser, N., Squires, G., Broadhurst, T., 1995, ApJ, 449, 460
 Lin, Huan, Yee, H. K. C., Carlberg, R. G., Morris, S. L., Sawicki, M., Patton, D. R., Wirth, G., Shepherd, C. W., 1999, ApJ, 518, 533
 Luppino, G. A., Kaiser, N., 1997, ApJ, 475, 20
 Marinoni, C., Hudson, M.J., 2002, ApJ, 569, 101
 Mellier, Y., 1999, ARA&A, 37, 127
 Miralda-Escudé, J., 1991, ApJ, 370, 1
 Navarro, Julio F., Frenk, Carlos S., White, Simon D. M., 1996, ApJ, 462, 563
 Press, W. H., Schechter, P., 1974, ApJ, 187, 425
 Ramella, Massimo, Pisani, Armando, Geller, Margaret J., 1997, AJ, 113, 482
 Sanderson, A. J. R., Ponman, T. J., 2003, MNRAS, 345, 1241
 Sheldon, E. S. et al., 2002, ApJ, 554, 881
 Tucker, Douglas L., Oemler, Augustus, Jr., Hashimoto, Yasuhiro, Shectman, Stephen A., Kirshner, Robert P., Lin, Huan, Landy, Stephen D., Schechter, Paul L., Allam, Sahar S., 2000, ApJS, 130, 237
 Valdes, F. G., 1997, Astronomical Data Analysis Software and Systems VI, 125, 455
 van den Bosch, Frank C., Yang, Xiaohu, Mo, H.J., 2003, MNRAS, 340, 771
 Wright, C. O., Brainerd, T. G., 2000, ApJ, 534, 34
 Yee, H. K. C., Morris, S. L., Lin, H., Carlberg, R. G., Hall, P. B., Sawicki, M., Patton, D. R., Wirth, G. D., Ellingson, E., Shepherd, C. W., 2000, ApJS, 129, 475